Properties of $[Mg_2(thd)_4]$ as a Precursor for Atomic Layer Deposition of MgO Thin Films and Crystal Structures of $[Mg_2(thd)_4]$ and $[Mg(thd)_2(EtOH)_2]$

Timo Hatanpää, Jarkko Ihanus, Jarno Kansikas, Ilpo Mutikainen, Mikko Ritala, and Markku Leskelä*

Department of Chemistry, Laboratory of Inorganic Chemistry, University of Helsinki, P.O. Box 55, FIN-00014 Helsinki, Finland

Received January 28, 1999. Revised Manuscript Received April 30, 1999

Complexes $[Mg_2(thd)_4]$ (**1**) and $[Mg(thd)_2(EtOH)_2]$ (**2**) (Hthd = 2,2,6,6-tetramethyl-3,5-heptanedione) were prepared and characterized using various techniques, viz. X-ray diffraction, NMR and mass spectroscopy, and thermal analysis. Crystal structures of compounds **1** and **2** were determined. Complex **1** crystallizes as a dimer where three oxygen atoms from three different thd ligands join the Mg atoms together. Crystallization from ethanol results in a monomeric complex having solvent coordinated to Mg. Both complexes volatilize completely, but in **2**, coordinated ethanol molecules do not stay intact in the gas phase. Complex **1** was used with H_2O_2 as precursors in the growth of MgO thin films by atomic layer deposition techniques. A rather constant growth rate of 0.10−0.14 Å/cycle was observed at 325−425 °C.

Introduction

Volatile compounds of alkaline earth metals have been the subject of great interest because they are needed for preparing many technologically interesting thin films by chemical vapor deposition (CVD) and related methods, like atomic layer deposition (ALD), which is also known as atomic layer epitaxy (ALE).[1−3] Most of this interest has been devoted toward the heavier elements Ca, Sr, and Ba, while Mg has gotten less attention.[4,5] A majority of this research has focused on β-diketonate compounds and their adduct derivatives, though also cyclopentadienyl compounds have been examined.

The chemistry of the alkaline earth β-diketonate compounds is dominated by the fact that in the monomeric M(β-diketonato)$_2$ the coordination number of the metal would be only four, whereas these metals prefer higher coordination numbers. To compensate for the coordination unsaturation, the compounds either oligomerize or react with solvent or impurities, like water. These reactions may take place slowly during the storage or use in the process and thereby cause undesired aging, i.e., changes in the precursor properties, especially in their volatility. Because of the smaller size of the Mg^{2+} ion, it prefers lower coordination numbers than the heavier alkaline earth metals, and thus it could be thought that the desired precursor properties—good volatility and resistance against aging—would be much easier to achieve. However, like the heavier alkaline earth elements, also magnesium tends to form oligomeric β-diketonate complexes which are reactive against small Lewis base molecules such as H_2O. This behavior is reflected in unidentical characteristics reported for "Mg(thd)$_2$" when different synthesis methods and storage conditions have been used.[6−9]

MgO thin films can be used in several applications such as buffer layers for ferroelectric and superconducting films, protecting layer in plasma displays, and as a part of oxide thin films for gas sensors.[10] MgO thin films can be prepared by different methods, like electron beam evaporation,[11] laser ablation,[12] molecular beam epitaxy,[13] sol−gel,[14] spray pyrolysis,[15] sputtering,[16] chemical vapor deposition (CVD)[17−24] and atomic layer deposition.[25] As already noted, in CVD β-diketonates have been the most important precursors and there are a

(1) Suntola, T. *Thin Solid Films* **1992**, *216*, 84.
(2) Leskelä, M.; Ritala, M. *J. Phys. Paris IV* **1995**, *5*, C5−937.
(3) Niinistö, L.; Ritala, M.; Leskelä M. *Mater. Sci. Eng.* **1996**, *B41*, 23.
(4) Wojtczak, W. A.; Fleig, P. F.; Hampden-Smith, M. J. *Adv. Organomet. Chem.* **1996**, *40*, 215.
(5) Tiitta, M.; Niinistö, L. *Chem. Vap. Depos.* **1997**, *3*, 167.
(6) Schwarberg, J. E.; Sievers, R. E.; Moshier, R. W. *Anal. Chem.* **1970**, *42*, 1828.
(7) Arunasalam, V.-C.; Drake, S. R.; Hursthouse, M. B.; Malik, K. M. A.; Miller, S. A. S.; Mingos, D. M. P. *J. Chem. Soc., Dalton Trans.* **1996**, 2435.
(8) Hammond, G. S.; Nonhebel, D. C.; Wu, C.-H., S. *Inorg. Chem.* **1963**, *2*, 73.
(9) Berg, E. W.; Herrera, N. M. *Anal. Chim. Acta* **1972**, *60*, 117.
(10) Miyata, T.; Minami, T.; Shimokawa, K.; Kakumu, T.; Ishii, M. *J. Electrochem. Soc.* **1997**, *144*, 2432.
(11) Chang, L. D.; Tseng, M. Z.; Hu, E. L.; Fork, D. K. *Appl. Phys. Lett.* **1992**, *60*, 1753.
(12) Tiwari, P.; Sharan, S.; Narayan, J. *J. Appl. Phys.* **1991**, *69*, 8358.
(13) Yadavalli, S.; Yang, M. H.; Flynn, C. P. *Phys. Rev. B.* **1990**, *41*, 7961.
(14) Rywak, A. A.; Burlitch, J. M.; Loehr, T. M. *Chem. Mater.* **1995**, *7*, 2028.
(15) DeSisto, W. J.; Henry, R. L. *Appl. Phys. Lett.* **1990**, *56*, 2522.
(16) Tonouchi, M.; Sakaguchi, Y.; Kobayashi T. *J. Appl. Phys.* **1987**, *62*, 961.
(17) Kwak, B. S.; Boyd, E. P.; Zhang, K.; Erbil, A.; Wilkins, B. *Appl. Phys. Lett.* **1989**, *54*, 2542.
(18) Zhao, Y.-W.; Suhr, H. *Appl. Phys. A* **1992**, *54*, 451.
(19) Lu, Z.; Feigelson, R. S.; Route, R. K.; DiCarolis, S. A.; Hiskes, R.; Jacowitz, R. D. *J. Cryst. Growth* **1993**, *128*, 788.

10.1021/cm991008e CCC: $18.00
Published on Web 06/29/1999

number of reports on the use of $Mg(thd)_2$ (thd = 2,2,6,6-tetramethyl-3,5-heptanedionato),[17−20] $Mg(acac)_2$ (acac = acetylacetonato),[21−23] and alkoxide Mg(2-ethylhexanoate)[24] complexes together with H_2O or O_2 to deposit MgO. In ALD, however, only $MgCp_2$ (Cp = cyclopentadienyl), together with H_2O, has been used.[25]

In this paper we report the synthesis, thermal behavior, spectroscopic properties, and crystal structures of $[Mg_2(thd)_4]$ (**1**) and $[Mg(thd)_2(EtOH)_2]$ (**2**) complexes. We also describe the precursor properties of **1** in ALD growth of MgO thin films.

Experimental Section

General Methods. All starting materials for synthesis of **1** were used as purchased. Because of possible adduct formation and decomposition of **1**, all manipulations after drying and sublimation of the product were made under dry conditions using standard glovebox and Schlenk techniques. Ethanol (>99.6%) used for crystallization was further dried with magnesium. Melting points were recorded with an electrothermal melting point apparatus using capillaries open to air. Elemental analyses (C, H, N) were performed at the University of Oulu in the Trace Elements Laboratory. The NMR spectra were recorded on a Varian Gemini 2000 spectrometer at ambient temperature. Chemical shifts referenced to tetramethylsilane are given in ppm. Mass spectra were recorded by with a JEOL JMS-SX102 operating in electron impact mode (70 eV) using a direct insertion probe and a temperature range of 50−200 °C. A Mettler Toledo TA8000 system equipped with a TGA850 thermobalance was used for thermal analyses of the samples under flowing nitrogen atmosphere. In dynamic experiments the samples investigated were between 10 and 11 mg and the heating rate was 10 °C min^{-1}. In isothermal mass change determinations, sample sizes were approximately 20 mg. Samples were heated at constant temperature for 20 min. Then the temperature was increased 40 °C and the isothermal stage was repeated.

Synthesis of $[Mg_2(thd)_4]$ (1). The complex **1** was prepared in an aqueous media by the previously reported method.[6] After synthesis the crude product was dried in a vacuum in the presence of P_2O_5 for 15−20 h and purified by sublimation at approximately 120 °C/0.2 mbar. Sublimation resulted in clear or white glasslike material. The product was collected in a glovebox and stored in a freezer at − 20 °C. Crystals suitable for X-ray analysis were obtained by dissolving the sublimated product in *n*-hexane and allowing the solvent to slowly evaporate in a N_2 atmosphere in a glovebox. Yield after sublimation was 40−71%. Mp 122−126 °C. Anal. Calcd for $MgC_{22}H_{38}O_4$ (390.85): C, 67.61; H, 9.80. Found: C, 67.25; H, 10.47. ^1H NMR ($CDCl_3$) δ 1.09 (36H, m, CH_3), 5.65 (2H, s, CH); $^{13}C\{^1H\}$ NMR 28.27 (CH_3), 28.42 (CH_3), 28.83 (CH_3), 40.96 ($C(CH_3)$), 91.80 (CH), 201.43 (CO); MS (EI, 70 eV) *m*/*z* 781 $[Mg_2(thd)_4]^+$, 597 $[Mg_2(thd)_3]^+$, 390 $[Mg(thd)_2]^+$, 375 $[Mg(thd)_2 - Me]^+$, 333 $[Mg(thd)_2 - tBu]^+$, 207 $[Mg(thd)]^+$.

Synthesis of $[Mg(thd)_2(EtOH)_2]$ (2). The adduct was prepared by dissolving the sublimated **1** in dry ethanol and allowing the solvent to slowly evaporate in a N_2 atmosphere in a glovebox. After collecting and washing the crystals with a small amount of ethanol, they were dried in a vacuum. Mp 64 °C. Anal. Calcd for $MgC_{26}H_{50}O_6$ (483,00): C, 64.66; H, 10.43. Found: C, 64.23; H, 10.63. ^1H NMR ($CDCl_3$) δ 1.07 (36H, s, CH_3), 1.20 (6H, t, CH_3), 3.71 (4H, q, CH_2), 5.61 (2H, s, CH); $^{13}C\{^1H\}$ NMR 18.10 (CH_3, EtOH) 28.35 (CH_3), 40.83 ($C(CH_3)$), 58.50 (CH_2, EtOH), 90.56 (CH), 200.79 (CO); MS (EI, 70 eV) *m*/*z* 781 $[Mg_2(thd)_4]^+$, 597 $[Mg_2(thd)_3]^+$, 390 $[Mg(thd)_2]^+$, 375 $[Mg(thd)_2 - Me]^+$, 333 $[Mg(thd)_2 - tBu]^+$, and 207 $[Mg(thd)]^+$.

Single-Crystal X-ray Structure Determination. For both compounds a single-crystal was mounted on a four-circle Rigaku AFC-7S diffractometer on a glass fiber using the viscous oil-drop method at 193 K.[26] Radiation used was graphite-monochromated Mo Kα (λ = 0.71073 Å). Unit cell parameters were determined by centering 25 reflections found by the search method. Data collections were done using the $\omega-2\theta$ scan method and intensities were extracted using the Lehmann−Larsen method,[27] included in the AFC-7S diffractometer control software.[28] Three standard reflections for both compounds were recorded after every 200 collected reflections. No decay was observed for either crystal, but about 1% random intensity fluctuations in test reflections were found. Intensities were corrected for Lorentz and polarization effects and space groups were determined using the TEXSAN program system.[29] Absorption was checked using an empirical ι-scan method, but no corrections were made due to the small variations in relative transmission scaled to T_{max} = 1.0 (T_{min} = 0.977 for **1** and 0.982 for **2**), and hence the maximum loss in intensities for **1** and **2** are 2.2 and 1.7%, respectively. Structures were solved with the SIR92[30] program, and further refinements were carried out using the SHELXL-93[31] software package. Illustrations were produced by the SHELXTL-PC[32] program.

ALD Film Growth Experiments. The film growth experiments were carried out using a commercial hot-wall flow type F-120 reactor (Microchemistry Ltd., Finland)[1] operating under a nitrogen pressure of 10 mbar. MgO films were deposited by pulsing sequentially complex **1** and H_2O_2 (Riedel-de Haën, 30%) on 5 × 5 cm^2 soda lime glass substrates using N_2 (99,999%) as a carrier and purging gas. Complex **1** was evaporated at 110 °C from an open boat inside the reactor and it was pulsed on the substrates by means of inert gas valving.[1] Use of evaporation temperatures higher than 110 °C for **1** was also feasible, and thereby it was in some cases possible to reach a somewhat higher growth rate for MgO. In those cases, however, the consumption of **1** increased unreasonably, thus preventing the use of evaporation temperatures higher than 110 °C in our experiments. A solenoid valve was used to pulse H_2O_2 in to the reactor from an external glass bottle held at room temperature.

Film thicknesses and refractive indices were evaluated by fitting transmittance spectra using a procedure developed by Ylilammi and Ranta-aho.[33] The spectra were measured in the wavelength region of 370−1100 nm. Film crystallinity was examined with a powder X-ray diffractometer using Cu Kα radiation.

Results and Discussion

Synthesis. Complex **1** was prepared by the previously reported method:[6] an aqueous ethanoic solution of $MgSO_4$ was reacted with Na(thd). The complex produced was then filtered from the solution, dried in a vacuum, and purified by vacuum sublimation, which

(20) Dean, K. A.; Buchholz, D. B.; Marks, L. D.; Chang, R. P. H.; Vuchic, B. V.; Merkle, K. L.; Studebaker, D. B.; Marks, T. J. *J. Mater. Res.* **1995**, *10*, 2700.
(21) Kamata, K.; Shibata, Y.; Kishi, Y. *J. Mater. Sci. Lett.* **1984**, *3*, 423.
(22) Fujii, E.; Tomozawa, A.; Fujii, S.; Torii, H.; Takayama, R.; Hirao, T. *Jpn. J. Appl. Phys.* **1994**, *33*, 6331.
(23) Zeng, J. M.; Wang, H.; Shang, S. X.; Wang, Z.; Wang, M. *J. Cryst. Growth* **1996**, *169*, 474.
(24) Maruyama, T.; Shionoya, J. *Jpn. J. Appl. Phys.* **1990**, *29*, L810.
(25) Huang, R.; Kitai, A. H. *J. Electron. Mater.* **1993**, *22*, 215.
(26) Kottke, T.; Stalke, D. *J. Appl. Crystallogr.* **1993**, *26*, 615.
(27) Lehmann, M. S.; Larsen, F. K. *Acta Crystallogr., Sect A30* **1974**, 580.
(28) *MSC/AFC Diffractometer Control Software*; Molecular Structure Corporation: The Woodlands, TX 77381, 1992.
(29) *TEXSAN: Single-Crystal Structure Analysis Software*; Molecular Structure Corporation: The Woodlands, TX 77381, 1993.
(30) Burla, M. C.; Camalli, M.; Altomare, A.; Cascarano, G.; Giacovazzo, C.; Guagliardi, A. *SIR92*, XIV European Crystallographic Meeting, Enschede, The Netherlands, 1992.
(31) Sheldrick, G. M. *SHELXL-93, Program for the Refinement of Crystal Structures*; University of Göttingen, Germany, 1993.
(32) Sheldrick, G. M.*SHELXTL-PC, Release 4.1*; Siemens Analytical X-ray Instruments Inc.: Madison, WI 53719, 1990.
(33) Ylilammi, M.; Ranta-aho, T. *Thin Solid Films*, **1993**, *232*, 56.

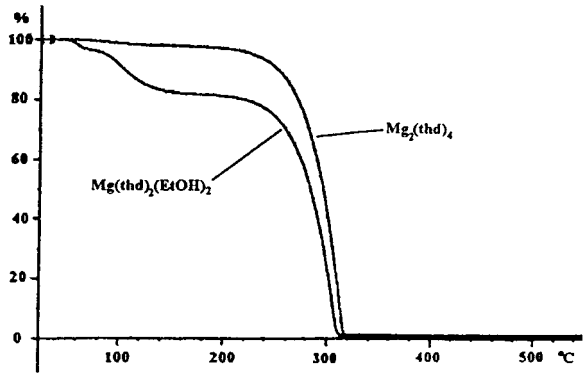

Figure 1. TG curves of $[Mg_2(thd)_4]$ and $[Mg(thd)_2(EtOH)_2]$.

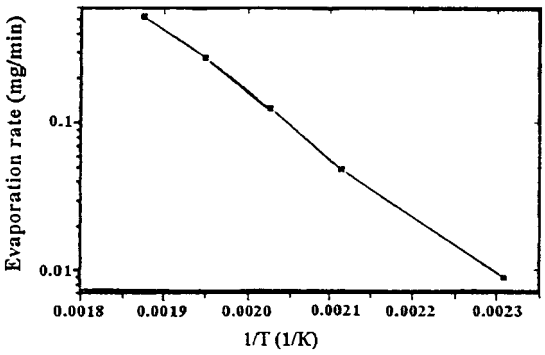

Figure 2. Evaporation rate of $[Mg_2(thd)_4]$ as function of $1/T$.

resulted in clear or white glasslike material. The yields of the raw product were close to 100%, but the sublimation yields varied between 40 and 71% from batch to batch. The low sublimation yields and the slight stickiness of the sublimated product are probably due to the fact that the product from the synthesis in the aqueous media is water adducted, and during drying or sublimation part of the adducted product reacts with the H_2O ligands, liberating Hthd and forming involatile compounds which contain oxo and/or hydroxo groups. Another possibility is that the synthesis product already contains involatile material with oxo and/or hydroxo groups. The raw product was not analyzed. Since no X-ray diffraction was observed, the material obtained from the sublimation was not suitable for single-crystal X-ray analysis, but after crystallization in *n*-hexane, crystals identified as $[Mg_2(thd)_4]$ (**1**) were obtained. All the analysis (mp, NMR, TG, DSC, MS, elemental analyses) pointed out that the molecular structures are most probably the same for the amorphous material obtained from the sublimation and the crystals crystallized from *n*-hexane. Some characteristics, like melting point of $[Mg_2(thd)_4]$, were found to be different from those found for "$Mg(thd)_2$" prepared earlier by other authors.[6−9] For example, melting points reported for "$Mg(thd)_2$" have been 60−65,[6] 94,[8] 94−95,[9] and 255−265 °C[7] while our product melted at 122−126 °C. The large spread of the melting points is apparently due to different synthesis methods and handling resulting in different kind of products. Some products may have contained oxo or hydroxo groups that caused oligomerization, while in some products there may have been small quantities of Hthd, water, or ethanol coordinated to Mg.

The complex **2** was obtained by dissolving **1** in ethanol and allowing the solvent to evaporate slowly. The single crystals obtained were identified as $[Mg(thd)_2(EtOH)_2]$, and they had much lower melting point of 64 °C compared to 122−126 °C for $[Mg_2(thd)_4]$.

Thermal Analyses. TG and DTG curves of **1** and **2** are presented in Figure 1. The complex **1** evaporates almost completely in one step, as reported earlier,[6] leaving a residue of only 0.49%. By contrast, the TG curve of **2** contains three steps, the first step being associated with a loss of uncoordinated EtOH (mass loss measured 3.68%), the second step with evaporation of two coordinated ethanol molecules (mass loss measured 14.63%, calculated 18.71%), and the third one with evaporation of $[Mg_2(thd)_4]$ dimer (residue of 1.00%). Evaporation of $[Mg_2(thd)_4]$ (**1**) takes place in the temperature range 200−318 °C ($T_{50\%}$ = 294 °C). The TG curves of the sublimated and crystallized $[Mg_2(thd)_4]$ (**1**) complexes are identical. It is worth noting here that even if $[Mg(thd)_2(EtOH)_2]$ (**2**) does not sublime as such but first decomposes into $[Mg_2(thd)_4]$, it still may give an advantage over $[Mg_2(thd)_4]$ in terms of better stability against aging during storage, thereby ensuring constant precursor properties in CVD or ALD.

Isothermal TG experiments were made for **1** in order to get information on evaporation rates at different temperatures and to detect possible decomposition. The results of these experiments are shown in Figure 2, where the evaporation rate is represented in a logarithmic scale as a function of $1/T$. The linearity of this plot reflects the pure sublimation or evaporation in absence of thermal decomposition. The deviation from the linearity at low temperatures is probably due to moisture in the samples.

Mass Spectra. The mass spectra of **1** and **2** are similar. The molecular peak for $[Mg(thd)_2(EtOH)_2]$ (**2**) was not observed, as can be understood on basis of the adduct ligand detachment during sublimation (Figure 1). The most intense peak in both mass spectra is due to $[Mg(thd)_2 - C(CH_3)_3]^+$ at *m*/*z* 333. A peak from $[Mg(thd)_2]^+$ and small peaks assigned to dimeric species $[Mg_2(thd)_4]^+$ (*m*/*z* 781) and $[Mg_2(thd)_3]^+$ (*m*/*z* 597) are also observed in the spectra. Besides these peaks, peaks originating from other fragments of the complex and thd can be seen. In the mass spectrum of the ethanol adduct **2**, peaks originating from ethanol are observed as well.

NMR Spectra. In the ^1H NMR spectrum of **1** the peaks are shifted to higher field compared to the free Hthd, which gives peaks at 1.18 and 5.74 ppm relative to tetramethylsilane. The peak originating from the methyl protons of the thd ligands at 1.09 ppm is split into a quintet, and the peak originating from the methine protons at 5.65 is not split. The observed split is probably due to the dimeric structure of the complex. In the spectrum of **2** both the methyl and the methine protons give a sharp singlet peak slightly shifted to higher field (1.07 and 5.61 ppm) as compared with the free Hthd and $[Mg_2(thd)_4]$. Likewise the methyl peaks originating from the adduct ethanol ligands were shifted to higher field (1.20 ppm) as compared with free EtOH, which gives methyl peaks at 1.23. Peaks from the CH_2 protons of ethanol are shifted to lower field (3.71 ppm) from their usual positions (3.69 ppm).

In the proton decoupled ^{13}C spectrum of **1** there are three different peaks originating from the methyl carbons, while only one peak originates from each of the

Table 1. Crystal Data and Structure Refinement for [Mg(thd)$_2$(EtOH)$_2$] (1) and [Mg$_2$(thd)$_4$] (2)

parameter	1	2
empirical formula	$C_{44}H_{76}Mg_2O_8$	$C_{26}H_{50}MgO_6$
formula weight	781.67	482.97
temp, K	193(2)	193(2)
λ(Mo Kα), Å	0.71073	0.71073
crystal system	monoclinic	triclinic
space group	$P2_1/c$ (No. 14)	$P\bar{1}$ (No. 2)
a, Å	14.212(3)	16.275(5)
b, Å	15.926(3)	10.461(5)
c, Å	22.177(4)	18.801(5)
α, deg		90.210(5)
β, deg	101.50(3)	110.630(5)
γ, deg		89.760(5)
V (Å^3), Z	4919(2), 4	2996(2), 4
d_{calc}, Mg/m^3	1.056	1.071
μ, mm^{-1}	0.093	0.092
F(000)	1712	1064
Crystal size, mm	0.25 × 0.30 × 0.35	0.35 × 0.40 × 0.40
θ range, deg	2.56−24.00	2.67−22.52
limiting indices	$0 \le h \le 15$	$0 \le h \le 16$
	$0 \le k \le 18$	$-11 \le k \le 10$
	$-25 \le l \le 24$	$-18 \le l \le 18$
reflections collected	5540	5326
independent reflections	5540 [R(int) = 0.0000]	3184 [R(int) = 0.1217]
no. of reflections [$F_o > 4\sigma(F)$]	2920	2142
refinement method	full-matrix least-squares on F^2	
data/parameters	5482/488	3129/299
goodness-of-fit on F^2	1.014	1.011
final R indices [$I > 2\sigma(I)$][a]	$R_1 = 0.1359$, $wR_2 = 0.3101$	$R_1 = 0.0855$, $wR_2 = 0.1963$
R indices (all data)	$R_1 = 0.2071$, $wR_2 = 0.3734$	$R_1 = 0.1300$, $wR_2 = 0.2726$
extinction coefficient	0.0004(9)	0.0002(7)
max/min diff peak,e Å^{-3}	0.801/−0.602	0.687/−0.364

[a] $R_1 = \sum||F_o| - |F_c||/\sum|F_o|$, $wR_2 = \{\sum[w(F_o^2 - F_c^2)^2]/\sum[w(F_o^2)^2]\}^{1/2}$.

other kind of carbon atoms (cf. Experimental Section). The three peaks originating from the methyl carbons indicate that there are three different kinds of chemical environments around methyl groups. In the ^{1}H-decoupled ^{13}C spectra of **2**, only one peak originating from each kind of carbon is observed, thus implying, in good accordance with the ^{1}H NMR spectrum, that in the monomeric complex **2** the methyl groups of thd have similar chemical environments.

When the complex **1** is exposed to air, the ^{1}H spectrum changes so that two peaks originating from the methyl (1.04 and 1.18 ppm) and the methine (5.73 and 5.49 ppm) protons appear. Besides this, peaks originating from the methyl protons change to a sharp singlet. Though the other peaks (1.18 and 5.73 ppm) are observed approximately at the places where peaks from the free Hthd should appear, the spectrum cannot be explained simply by decomposition of the complex to Hthd and hydroxo- and/or oxo-group-containing complex because in the TG measurements the complex evaporates completely: it first releases water and then [Mg$_2$(thd)$_4$] evaporates approximately at the same temperature region as the fresh compound. An explanation for these observations could be that the water adduct which forms during exposure to moist air splits the signal because of its structure or that two different kind of water adducts form. From the practical point of view a positive observation is that the evaporation behavior of the original [Mg$_2$(thd)$_4$] (**1**) seems to be recovered once the water is first evaporated. Hence the compound exposed to air should give similar delivery rates as the fresh [Mg$_2$(thd)$_4$] in CVD or ALD processes.

Single-Crystal X-ray Structures. A crystal structure determination summary is presented in Table 1. Figures 3 and 4 show structures and atomic labeling

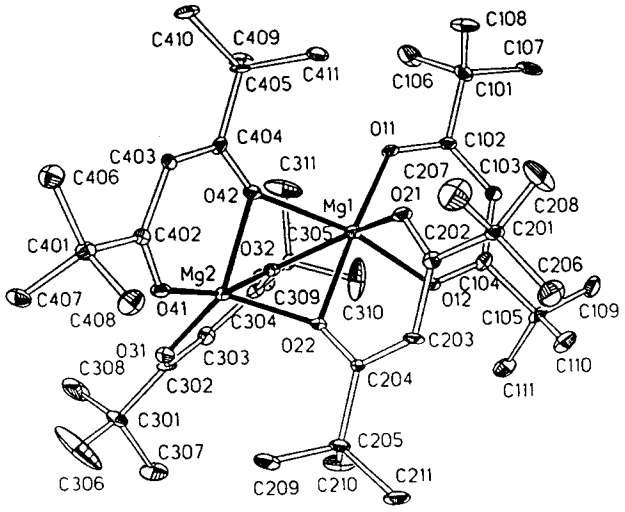

Figure 3. View of [Mg$_2$(thd)$_4$] (**1**) with atomic labeling. Ellipsoids are drawn on the 30% probability level. H atoms are omitted for clarity.

for **1** and **2**, respectively. Atomic coordinates and equivalent isotropic displacement parameters for nonhydrogen atoms are listed in Tables 2 and 3, respectively. Table 4 gives selected interatomic distances for **1** and **2**, respectively, including also a nonbonded Mg1−Mg2 distance of 2.818(4) Å in **1**. Table 5 lists selected bond angles.

The structure of **1** shows that Mg(thd)$_2$, when crystallized from nonpolar solvent, oligomerizes. When the larger alkaline earth metal thd chelates are crystallized from nonpolar solvent, trimers (Ca,[7] Sr[34]) and tetramers

(34) Drake S. R.; Hursthouse, M. B.; Malik, K. M. A.; Otway, D. J. *J. Chem. Soc., Dalton Trans.* **1993**, 2883.

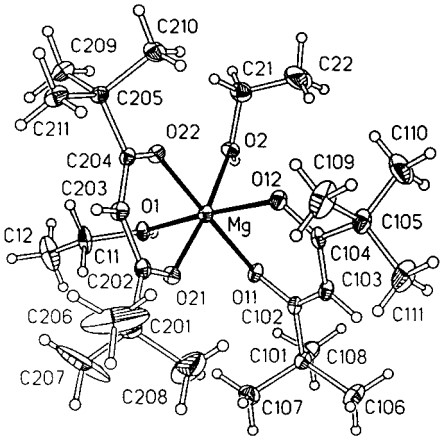

Figure 4. View of $[Mg(thd)_2(EtOH)_2]$ **2** with atomic labeling. Ellipsoids are drawn on the 30% probability level. H atoms are shown as circles of fixed radii.

(Ba)[34] are formed. Pentamers and hexamers of Ba are also known.[35−38] The oligomerization behavior can be well-understood in terms of the coordinative unsaturation and the preferred coordination numbers of the metals that increase with increasing size. Because of the smaller size $Mg(thd)_2$ forms only a dimer. Sterically less demanding β-diketonato ligands such as acetylacetonato or ethylacetoacetato form trimeric Mg complexes when there is no other molecules capable to coordinate.[39,40] Ethanol is capable of breaking the $[Mg_2(thd)_4]$ dimer, and a monomeric complex is formed, as proven by the crystal structure of **2**. In the case of Ca, the ethanol adducted β-diketonato complex $[Ca_2(thd)_4(EtOH)_2]$ is dimer.[7] This is due to the insufficient separation between the two $Ca(thd)_2(EtOH)$ units. It seems that ethanol molecules are not capable of coordinating to oligomeric $Ca_x(thd)_{2x}$ to such an extent as monomers, like $[Ca(thd)_2(EtOH)_2]$, are.

In **1** the two magnesium atoms have different kinds of coordination around them and the complex is thus unsymmetrical. Mg1 has six coordination and Mg2 five coordination. Only one thd ligand is bidentately coordinated to Mg1. In the other three thd ligands, one of the oxygen atoms is coordinated also to the neighboring Mg atom, forming three oxygen bridges between Mg atoms. Coordination around Mg in **2** is a distorted octahedral, where the distances of Mg to oxygen atoms of the ethanol molecules are slightly longer than to the keto oxygens. The ethanol ligands occupy cis positions in the coordination sphere. In **1** coordination at Mg1 yields a more distorted octahedral than in **2**. Mg2 is trigonal bipyramidally distorted square-pyramidal with the angle of 163.5° referring to the O32−Mg2−O41 angle formed by atoms at apical positions.

The atoms O*n*1−C*n*02−C*n*03−C*n*04−O*n*2 (n = 1−4 for **1** and n = 1,2 for **2**) of thd molecules form a plane with mean deviations from planarity of 0.007(7) to 0.043(7) Å for **1** and 0.024(4) and 0.006(4) Å for **2**. These planes are tilted from the O−Mg−O bite planes from 2.6(3) to 32.3(4)° for **1** and 27.1(2) and 12.7(2)° for **2**. For **1**, deviations of Mg1 from the thd ls planes where n = 1 and 2 are 0.296(7) and 0.835(7) Å, respectively. Deviation of Mg2 is 0.064(7) and 0.254(7) Å from the planes with n = 3 and 4, respectively. This indicates that for five-coordinated Mg2 sterical hindrance is smaller and also the deviations from planarity are smaller. Strong sterical hindrance around Mg1 may also yield to the poor crystal quality. In **2**, Mg deviates

Table 2. Atomic Coordinates (×10⁴) and Equivalent Isotropic Displacement Parameters (Å² × 10³) for $[Mg_2(thd)_4]$ (1)

atom	*x*	*y*	*z*	U_{eq}[a]
Mg1	3225(2)	−922(2)	1839(1)	42(1)
Mg2	2265(2)	450(2)	2245(1)	40(1)
O11	4555(4)	−1292(4)	1822(3)	45(2)
O12	2812(4)	−1448(5)	1014(3)	47(2)
O21	2893(5)	−1951(4)	2282(3)	49(2)
O22	1785(4)	−610(4)	1843(3)	40(2)
O31	1723(5)	1496(4)	1904(3)	51(2)
O32	3125(4)	439(4)	1592(3)	42(2)
O41	1808(5)	532(5)	3012(3)	48(2)
O42	3431(5)	−187(4)	2705(3)	45(2)
C101	5892(8)	−2090(7)	1646(5)	59(3)
C102	4820(7)	−1825(7)	1469(5)	46(3)
C103	4239(7)	−2163(7)	956(5)	52(3)
C104	3268(9)	−1956(7)	740(5)	54(3)
C105	2649(8)	−2372(8)	158(4)	59(3)
C106	6488(9)	−1286(9)	1674(9)	111(6)
C107	6194(9)	−2705(10)	1192(6)	90(5)
C108	6023(9)	−2515(10)	2274(6)	90(5)
C109	3254(10)	−2893(9)	−197(6)	88(5)
C110	1915(9)	−2918(9)	387(6)	84(4)
C111	2167(11)	−1682(10)	−247(5)	95(5)
C201	2137(7)	−3255(7)	2411(5)	47(3)
C202	2120(8)	−2340(6)	2196(4)	40(2)
C203	1222(7)	−1968(7)	1882(5)	48(3)
C204	1084(7)	−1145(6)	1732(4)	38(2)
C205	126(7)	−775(7)	1428(5)	55(3)
C206	1313(13)	−3786(9)	2103(8)	120(6)
C207	2188(15)	−3229(11)	3092(7)	143(8)
C208	3022(13)	−3666(10)	2274(10)	135(7)
C209	−288(11)	−186(13)	1844(8)	152(9)
C210	263(10)	−303(11)	852(7)	111(6)
C211	−653(9)	−1437(9)	1205(8)	100(5)
C301	1296(9)	2723(8)	1292(6)	67(4)
C302	1912(7)	1919(7)	1461(4)	45(3)
C303	2601(9)	1736(7)	1133(5)	54(3)
C304	3195(7)	1018(7)	1198(4)	45(3)
C305	3946(8)	922(7)	826(5)	48(3)
C306	597(20)	2784(16)	1690(12)	264(20)
C307	755(14)	2673(12)	649(8)	159(9)
C308	1901(14)	3451(10)	1348(11)	153(9)
C309	4094(10)	1678(8)	432(6)	84(4)
C310	3725(16)	168(11)	422(9)	171(11)
C311	4932(10)	780(15)	1276(8)	147(9)
C401	1632(8)	483(7)	4055(4)	46(3)
C402	2187(7)	336(6)	3558(4)	37(2)
C403	3168(7)	11(6)	3705(4)	42(3)
C404	3709(7)	−214(6)	3302(4)	41(3)
C405	4744(7)	−539(7)	3517(4)	44(3)
C406	2190(9)	368(9)	4721(5)	75(4)
C407	1208(8)	1361(8)	3987(5)	63(3)
C408	814(9)	−147(8)	3934(6)	78(4)
C409	5382(8)	−128(8)	3145(6)	72(4)
C410	5126(9)	−349(9)	4204(5)	84(4)
C411	4734(8)	−1503(7)	3429(5)	60(3)

[a] U_{eq} is defined as one-third of the trace of the orthogonalized U_{ij} tensor.

(35) Turnipseed, S. B.; Barkley, R. M.; Sievers, R. E. *Inorg. Chem.* **1991**, *30*, 1164.
(36) Huang, L.; Turnipseed, S. B.; Haltiwanger, R. C.; Barkley, R. M.; Sievers, R. E. *Inorg. Chem.* **1994**, *33*, 798.
(37) Hovnanian, N.; Galloy, J.; Miele, P. *Polyhedron* **1995**, *14*, 297.
(38) Drozdov, A. A.; Troyanov, S. I.; Pisarevsky, A. P.; Struchkov, YU. T. *Polyhedron* **1994**, *13*, 2459.
(39) Weiss, E.; Kopf, J.; Gardein, T.; Corbelin, S.; Shümann U.; Kirilov, M.; Petrov, G. *Chem. Ber.* **1985**, *118*, 3529.
(40) Petrov, G.; Alexiev, A.; Angelova, O. *J. Coord. Chem.* **1992**, *25*, 101.
(41) Morosin, B. *Acta Crystallogr.* **1967**, *22*, 315.

Table 3. Atomic Coordinates ($\times 10^4$) and Equivalent Isotropic Displacement Parameters ($Å^2 \times 10^3$) for $[Mg(thd)_2(EtOH)_2]$ (2)[a]

atom	*x*	*y*	*z*	U_{eq}
Mg	8655(1)	4611(2)	5283(1)	33(1)
O1	9014(2)	4550(4)	4283(2)	36(1)
O2	9261(2)	6418(4)	5484(2)	37(1)
O11	9820(2)	3681(4)	5854(2)	36(1)
C11	8369(4)	4168(8)	3566(3)	61(2)
O12	8495(2)	4664(4)	6304(2)	43(1)
C12	8692(5)	4095(11)	2938(4)	108(4)
O21	7981(2)	2980(4)	4969(2)	38(1)
C21	8889(4)	7586(7)	5653(4)	59(2)
O22	7523(2)	5526(4)	4736(2)	36(1)
C22	9018(8)	7804(10)	6438(5)	144(5)
C101	10578(4)	1827(6)	6481(3)	41(2)
C102	9916(3)	2886(6)	6410(3)	35(2)
C103	9435(4)	2971(6)	6888(3)	41(2)
C104	8767(4)	3855(6)	6828(3)	38(2)
C105	8329(4)	3910(7)	7433(3)	55(2)
C106	10767(5)	1013(8)	7202(4)	71(2)
C107	10180(4)	967(7)	5788(4)	60(2)
C108	11450(4)	2356(7)	6481(4)	56(2)
C109	7329(4)	3964(10)	7012(4)	97(3)
C110	8661(6)	5131(10)	7894(5)	106(3)
C111	8522(5)	2763(9)	7957(4)	82(3)
C201	6857(4)	1407(6)	4687(4)	50(2)
C202	7159(4)	2805(6)	4730(3)	39(2)
C203	6542(4)	3791(6)	4507(3)	39(2)
C204	6744(4)	5082(6)	4509(3)	34(2)
C205	6424(3)	6121(6)	4235(3)	37(2)
C206	5943(6)	1256(10)	4685(11)	229(10)
C207	6992(14)	791(11)	4037(8)	275(12)
C208	7416(7)	725(10)	5380(6)	150(5)
C209	6219(4)	6938(6)	3631(4)	52(2)
C210	6109(4)	6969(7)	4925(4)	53(2)
C211	5089(3)	5603(7)	3902(4)	52(2)

[a] U_{eq} is defined as one-third of the trace of the orthogonalized U_{ij} tensor.

Table 4. Selected Interatomic Distances (Å) for $[Mg_2(thd)_4]$ (1) and $[Mg(thd)_2(EtOH)_2]$ (2)

1		2	
Mg1−O11	1.987(7)	Mg−O11	2.062(4)
Mg1−O12	1.992(7)	Mg−O12	2.027(4)
Mg1−O21	2.014(7)	Mg−O21	2.004(4)
Mg1−O22	2.109(7)	Mg−O22	2.007(4)
Mg1−O32	2.234(7)		
Mg1−O42	2.218(7)		
Mg2−O22	1.966(7)		
Mg2−O31	1.925(8)		
Mg2−O32	2.072(7)		
Mg2−O41	1.944(7)		
Mg2−O42	2.036(7)		
Mg1−Mg2	2.818(4)		
		Mg−O2	2.106(4)
		Mg−O1	2.156(4)
O11−C102	1.261(11)	O11−C102	1.302(6)
O12−C104	1.265(12)	O12−C104	1.257(7)
O21−C202	1.243(11)	O21−C202	1.265(6)
O22−C204	1.297(11)	O22−C204	1.276(6)
O31−C302	1.264(11)		
O32−C304	1.287(11)		
O41−C402	1.262(11)		
O42−C404	1.305(10)		
		O1−C11	1.443(6)
		O2−C21	1.445(8)

0.682(4) and 0.322(4) Å from the thd ls planes with $n =$ 1 and 2, respectively, compared to the value of 0.48 Å in diaquobis(acetylacetonato)magnesium(II).[41]

In **1**, Mg−O distances vary from very short, 1.925(8) Å, to relatively long, 2.234(7) Å, without clear dependence on the fact that the oxygen atoms can participate in bidentate coordination and also act as a bridging atom between the metal ions. In **2**, Mg−O distances are normal with a slightly longer Mg−O(ethanol) distance, which is similar to that found in bis(dimethylformamido)-bis(1,3diphenyl-1,3-propanedionato)magnesium.[42] Also Mg−O(H_2O) distances in the structure where water molecules lie at the apical positions the same elongation effect have been found compared to equatorial Mg−O(acac) distances.[41]

Table 5. Selected Interatomic Angles (deg) for $[Mg_2(thd)_4]$ (1) and $[Mg(thd)_2(EtOH)_2]$ (2)

1		2	
O11−Mg1−O12	88.0(3)	O11−Mg−O12	85.3(2)
O11−Mg1−O21	94.9(3)	O11−Mg−O21	93.5(2)
O11−Mg1−O22	176.3(3)	O11−Mg−O22	179.4(2)
O11−Mg1−O32	107.3(3)		
O11−Mg1−O42	102.2(3)		
O12−Mg1−O21	93.0(3)	O12−Mg−O21	93.4(2)
O12−Mg1−O22	89.7(3)	O12−Mg−O22	94.2(2)
O21−Mg1−O22	82.4(3)	O21−Mg−O22	86.9(2)
O12−Mg1−O32	100.9(3)		
O12−Mg1−O42	168.9(3)		
O21−Mg1−O32	154.1(3)		
O21−Mg1−O42	90.6(3)		
O22−Mg1−O32	76.0(3)		
O22−Mg1−O42	80.3(3)		
O32−Mg1−O42	72.0(3)		
O22−Mg2−O31	119.3(3)		
O22−Mg2−O32	82.9(3)		
O22−Mg2−O41	107.9(3)		
O22−Mg2−O42	88.5(3)		
O31−Mg2−O32	88.8(3)		
O31−Mg2−O41	96.2(3)		
O31−Mg2−O42	148.2(3)		
O32−Mg2−O41	163.5(3)		
O32−Mg2−O42	79.1(3)		
O41−Mg2−O42	88.5(3)		
		O1−Mg−O11	87.8(2)
		O1−Mg−O12	172.3(2)
		O1−Mg−O21	90.6(2)
		O1−Mg−O22	92.7(2)
		O2−Mg−O11	92.4(2)
		O2−Mg−O12	91.0(2)
		O2−Mg−O21	172.9(2)
		O2−Mg−O22	87.3(2)
		O1−Mg−O2	85.8(2)

ALD Growth of MgO. The aim of this part of the work was to demonstrate the use of $[Mg_2(thd)_4]$ (**1**) as a Mg precursor in the ALD growth of MgO. $[Mg(thd)_2(EtOH)_2]$ (**2**) was not used because the TG measurements indicated that when heated ethanol ligands detach first and the compound converts to $[Mg_2(thd)_4]$ **1**.

Figure 5 shows the growth rate of MgO as a function of growth temperature. Between 325 and 425 °C the growth rate is in practice independent of the growth temperature. The growth rate is, however, very low, which may be due to steric limitations between the adsorbed $Mg(thd)_x$ species, though also the low reactivity of $[Mg_2(thd)_4]$ or $Mg(thd)_2$, if the dimer is decomposed in the gas phase, toward the surface may be possible because the Mg ion is well shielded by the organic ligands. The growth rate increases at 450 °C, which is most probably due to decomposition of **1** (see below). However, above 450 °C the growth rate decreases again, which may indicate a desorption of the Mg precursor from the surface, which thereby competes and counter-

(42) Hollander, F. J.; Templeton, D. H.; Zalkin, A. *Acta Crystallogr.* **1973**, *B29*, 1289.

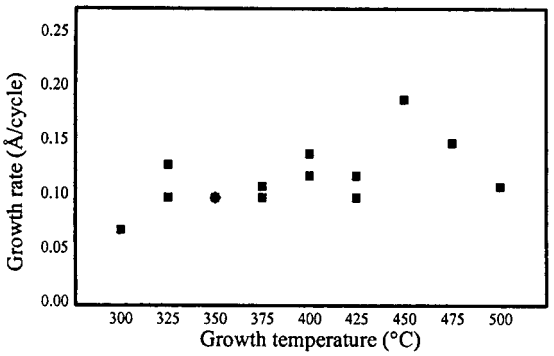

Figure 5. Growth rate of MgO in the center part of the substrate as a function of growth temperature. Pulse length for $[Mg_2(thd)_4]$ (**1**) complex and H_2O_2 was 1 s.

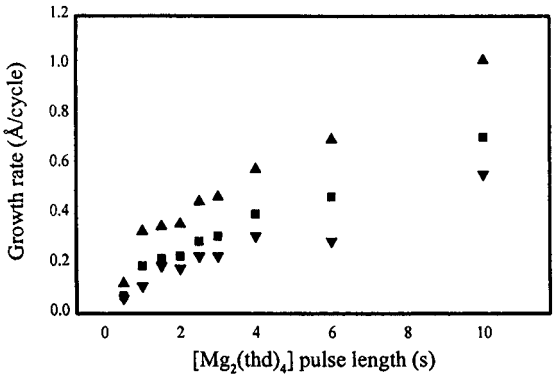

Figure 6. Growth rate of MgO as a function of $[Mg_2(thd)_4]$ (**1**) complex pulse length. Growth temperature was 450 °C and H_2O_2 pulse length was 1 s. Up triangles show the growth rate in the first part, squares in the middle, and down triangles in the latter part of the substrate along the flow direction.

balances the decomposition. The low growth rate at 325 °C is evidently due to a lack of thermal energy for surface reactions.

Figure 6 shows the growth rate of MgO as a function of $[Mg_2(thd)_4]$ (**1**) pulse length at 450 °C. The deposition rate increases continuously with increasing pulse length. The increase is fastest at short exposure times, which can be attributed to the desired chemisorption and surface reactions of $Mg(thd)_x$ with OH groups left on the surface after the preceding H_2O_2 dose. The slower increase at longer pulse times, in turn, is most probably due to self-decomposition of **1**, which is undesirable for an ideal ALD process because it destroys the self-limiting growth mechanism and thereby also increases the thickness profile across the substrate (Figure 6). Therefore, by using $[Mg_2(thd)_4]$ (**1**) pulse times around 2 s, one can maximize the contribution of the desired surface reactions and minimize that of the undesirable

(43) *CRC Handbook of Chemistry and Physics*, 54th ed; CRC Press: Cleveland, OH, 1973−74; p B-106.

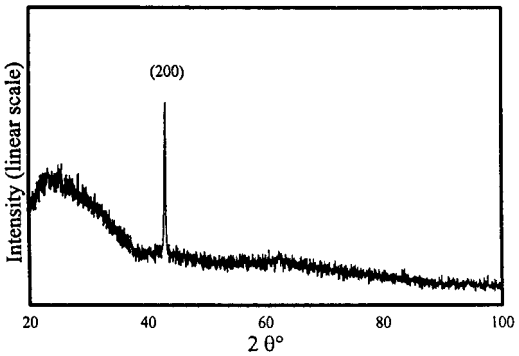

Figure 7. XRD diffractogram of the MgO film grown at 400 °C. The broad feature in the pattern is due to the glass substrate.

decomposition reactions at 450 °C. Under these conditions the process is not purely ALD; in a sense it is not self-limiting, but more like pulsed CVD.

It was interesting to note that complex **1** alone does not decompose to MgO at 450 °C since pulsing of only **1** did not result in any film growth. Apparently the MgO film formed in the reactions between **1** and H_2O_2 catalyzes the $[Mg_2(thd)_4]$ (**1**) decomposition.

Figure 7 shows a typical XRD diffractogram of the MgO film having the cubic structure. In all films only the (200) reflection was observed, thereby implying strong orientation in this direction. The refractive indices of the films were 1.7, which is close to the literature value[43] 1.736, indicating a dense structure of the films.

Conclusions

$Mg(thd)_2$ crystallizes as a dimer in nonpolar solvents. Mg atoms are joined together by three oxygen atoms. This type of bridging is also seen in $[Ca_3(thd)_6]$ molecule. Ethanol is capable of coordinating to Mg, and thus a monomeric $[Mg(thd)_2(EtOH)_2]$ complex is formed. Both complexes are volatile, but **2** first releases ethanols and after that $Mg(thd)_2$ sublimes. The mass spectra of the two complexes are similar. The thermal stability of **1** is good, enabling the ALD growth of MgO thin films at 325−425 °C. The growth rate is slow, however, around 0.1 Å/cycle. The MgO film shows strong (200) orientation.

Acknowledgment. This work was supported in part by Academy of Finland and Technology Development Centre (TEKES), Finland.

Supporting Information Available: Hydrogen atom coordinates, complete lists of bond lengths and angles, anisotropic displacement parameters, and listing of observed and calculated structure factors. This material is available free of charge via the Internet at http://pubs.acs.org.

CM991008E